A temporally constrained ICA (TCICA) technique for artery-vein separation of cerebral microvasculature

Hatef Mehrabian*[a,b], Liis Lindvere[a,b], Bojana Stefanovic[a,b] and Anne L. Martel[a,b]
[a]Department of Medical Biophysics, University of Toronto, Toronto, ON, Canada
[b]Imaging Research, Sunnybrook Health Sciences Centre, Toronto, ON, Canada

ABSTRACT

A fully automatic ICA based data driven technique which incorporates additional *a priori* information from physiological modeling of the cerebral microcirculation (gamma variate model) is developed for the separation of arteries and veins in contrast-enhanced studies of the cerebral microvasculature. A dynamic data set of 50 images taken by a two-photon laser scanning microscopy technique that monitors the passage of a bolus of dye through artery and vein is used here. A temporally constrained ICA (TCICA) technique is developed to extract the vessel specific dynamics of artery and vein by adding two constraints to classical ICA algorithm. One of the constraints guarantees that the extracted curves follow the gamma variate model of blood passage through vessels. Positivity as the second constraint indicates that none of the extracted component images that correspond to the artery, vein or capillaries in the imaging field of view, has negative impact on the acquired images.

Experimental results show improved performance of the proposed temporally constrained ICA (TCICA) over the most commonly used classical ICA technique (fast-ICA) in generating physiologically meaningful curves; they are also closer to that of pixel by pixel model fitting algorithms and perform better in handling noise. This technique is also fully automatic and does not require specifying regions of interest which is critical in model based techniques.

Keywords: Independent Component Analysis (ICA), Two Photon Laser Scanning Microscopy (2PLSM), Segmentation, Temporally Constrained ICA, Artery-Vein separation, Dynamic contrast enhanced imaging, Gamma variate model.

1. INTRODUCTION

A variety of CNS conditions – such as stroke, dementia, and epilepsy – involve a compromise in the responsivity of brain vasculature. In addition, the coupling of neuronal activity to the flow and volume of the surrounding brain vessels lies at the heart of modern neuroimaging methods such as functional MRI. The goal of this work is to characterize the spatial pattern of the cerebral microvascular network reactivity under physiological conditions. The current work investigates the transit of a fluorescent bolus through the 3D microvascular tree from high resolution two-photon laser scanning microscopy (2PLSM) volumes. Dynamic contrast enhanced (DCE) imaging of arteries and veins involves intravenously injecting a contrast agent (bolus of dye) and then repeatedly imaging the vessels to track the changes in contrast agent concentration over time [1]. The signal enhancement in the vessels, measured as a function of time after injection of the contrast agent contains functional information and reflects the response of the vascular system. Differentiation of artery and vein is performed based on the difference in the onset time, and time to peak of contrast concentration [2].

There exist two main categories of techniques for analyzing DCE image sequences, model based techniques and data driven techniques. The model based techniques are based on physiological models of the data. These models are generated based on the fact that the signal intensity (SI) of each pixel inside the vessels follows a gamma variate curve [3]. Thus, the SI curve of each pixel is fitted into the model and physiological parameters are extracted from the curves. These techniques are less sensitive to variations in acquisition protocol and also provide physiological meaning for the obtained parameters however they are very sensitive to noise and are time consuming [4].

Data driven techniques such as independent component Analysis (ICA), principal component analysis (PCA) and non-negative matrix factorization (NMF) are powerful tools for extracting functional information from dynamic image

Medical Imaging 2010: Biomedical Applications in Molecular, Structural, and Functional Imaging,
edited by Robert C. Molthen, John B. Weaver, Proc. of SPIE Vol. 7626, 762622 · © 2010 SPIE
CCC code: 1605-7422/10/$18 · doi: 10.1117/12.844913

sequences in a condensed manner [5]. Given a dynamic image sequence (a set of random variables), these techniques assume each pixel's time-intensity curve is constructed of a linear combination of a small number of time-intensity curves which we refer to here as physiological components. These components are associated with independent physiological structures [6-7]. These techniques use no assumption about the behavior of the contrast agent in the tissue and try to extract the main underlying features of the data set. They are capable of handling noise efficiently and are less time consuming compared to model based techniques, but their results are difficult to interpret since they may not represent any physiological feature. The data driven analysis technique that is used in this study is independent component analysis (ICA) which is a statistical technique that tries a find a linear transformation that maps the observed dynamic data into a set of statistically independent components [8].

The aim of this study is to develop a fully automatic artery-vein segmentation technique using a combination of model based and data driven techniques which takes benefit of the advantages of both techniques while minimizing their shortcomings. A temporally constrained ICA technique is developed to extract the main features of the dynamic data. The developed technique extracts the independent components (IC's) subject to positivity constraint (no IC is allowed to have negative impact on the resultant image) [9, 10] as well as a model fitting constraint (component curves follow gamma variate function). Section 2 describes the classical ICA techniques as well as the temporally constraint ICA (TCICA) technique that is developed in this study. In section 3 the experimental setup for acquisition of the cerebral microvasculature images of a rat brain is given. Section 4 talks about the results of applying the developed TCICA as well as a commonly used ICA technique (fast-ICA) and pixel by pixel model fitting techniques to the acquired DCE image data set. Section 5 presents discussion and also concluding remarks about the proposed method.

2. INDEPENDENT COMPONENT ANALYSIS

2.1. Classical Independent Component Analysis (fast-ICA)

Independent component analysis was first developed for blind source separation to estimate main components in the dataset that are statistically independent and construct the entire dataset. Given a set of M independent source signals $s(t) = \left[s_1(t), s_2(t), \ldots, s_M(t) \right]^T$ and N observed mixtures of the source signals $x(t) = \left[x_1(t), x_2(t), \ldots, x_N(t) \right]^T$ $(\text{usually } N \geq M)$, the noise-free linear ICA model is [7]:

$$x(t) = As(t) \tag{1}$$

Where A is an $N \times M$ mixing matrix. Having the observed signal $x(t)$, the goal of ICA is to estimate the source signals $\mathbf{s}(t)$ and the mixing matrix A. Classical ICA algorithms try to find an $M \times N$ unmixing matrix W as well as an estimate of the source matrix $y(t) = \left[y_1(t), y_2(t), \ldots, y_M(t) \right]^T$ such that:

$$y(t) = Wx(t) \tag{2}$$

where rows of $y(t)$ are statistically independent. In this model the sources can be recovered up to scaling and permutation. There is no straight method for finding independent components of a set of random variables. Thus IC's are calculated by maximizing the independence of the components through an optimization scheme.

Fast-ICA is an IC estimation algorithm based on maximizing non-Gaussianity of the estimated sources [11]. Based on the central limit theorem, the distribution of a sum of independent random variables tends towards a Gaussian distribution [12]. A robust measure of non-Gaussianity is Negentropy which is based on the information theoretic quantity of differential entropy. The differential entropy H of a random variable y with density $p_y(\eta)$ is defined as:

$$H(y) = -\int p_y(\eta) \log p_y(\eta) \, d\eta \tag{3}$$

Negentropy as a measure of non-Gaussianity of a signal y is defined as:

$$J(y) = H(y_{Gauss}) - H(y) \tag{4}$$

Where y_{Gauss} is a Gaussian random variable having zero mean and the same variance as the signal y [13]. Based on this definition, negentropy is always non-negative. It is also invariant for invertible linear transformations [8]. An estimate to negentropy, given in (4), is usually used for ICA purposes:

$$J(y) = \rho\left(E\{G(y)\} - E\{G(y_{Gauss})\}\right)^2 \tag{5}$$

where ρ is a positive constant and $G(\cdot)$ is a non-quadratic function. Various non-quadratic functions can be chosen for $G(\cdot)$ but to have a robust estimator it is recommended to use functions that do not grow fast [13]. The following function is used for $G(\cdot)$ in our algorithm.

$$G(y) = \log\left(\cosh(y)\right)$$

2.2. Temporally Constrained Independent Component Analysis (TCICA)

The one unit ICA-R algorithm developed by Lu *et al* [14] tries to find an $N \times 1$ unmixing vector w^* such that the output signal $y(t) = w^{*T}x(t)$ is equal to the desired source signal $s^*(t)$ subject to *a priori* information about $s^*(t)$. We have developed a similar algorithm in which the *a priori* information is, the component curves (columns of mixing matrix A), should take the form of a gamma variate function given in equation-6 [3]:

$$C(t) = \begin{cases} a & t < AT \\ a + K(t - AT)^{\alpha} e^{-(t-AT)/\beta} & t \geq AT \end{cases} \tag{6}$$

where t is time after injection, $C(t)$ is concentration at time t, K is a constant scale factor, a is the bias, AT is the appearance time and α, β are arbitrary parameters. The vessel specific dynamics are inferred from the parameters of this fitted gamma curve. The onset time of the contrast agent (bolus of dye) is equal to the appearance time of its gamma curve fit; the relationship between time-to-peak and gamma function parameters is $t_p = AT + \alpha\beta$.

As our constraint is on the mixing matrix **A** whereas the ICA technique operates on the unmixing matrix **W,** a transformation from mixing space to unmixing space is required. For an ideal separation $\mathbf{AW} = I$ and assuming that C' is the transformation of C into the space of the unmixing matrix **W**. The *a priori* constraint added to the ICA learning algorithm $\left(\varepsilon(w, C') = \|w - C'\|^2\right)$ is a measure of how well the estimated component curve fits the gamma variate function. Setting a threshold ζ, the desired closeness of the extracted component curve to its gamma fit is defined as

$$g(w) = \varepsilon(w, C') - \zeta \ .$$

The preprocessing step involves centering and whitening $x(t)$, the matrix of observed variables [15]. By adding the two constraints, $g(w)$ and positivity to the ICA cost function, the temporally constrained ICA algorithm is formulated as:

$$\begin{aligned} &\text{maximize} && J(y) \approx \rho\left(E\{G(y)\} - E\{G(y_{Gauss})\}\right)^2 \\ &\text{subject to} && g(w) \leq 0 \quad (\text{model fitting}) \\ &\& && y'(i) \geq 0 \quad (\text{Positivity}) \end{aligned} \tag{7}$$

Where y' is transformation of y into the space of un-whitened data. An augmented Lagrangian function for the problem is given by [16]:

$$L(w, \mu) = J(y) - \frac{1}{2\gamma}\left(\max^2\{\mu + \gamma g(w), 0\} - \mu^2\right) \tag{8}$$

where μ is the Lagrangian multiplier for model fitting constraint and γ is a scalar penalty parameter. The positivity constraint $\left(y'(i) \geq 0\right)$ is applied by truncating the negative part of the estimated IC at each iteration (this constraint is

not shown in the augmented cost functions). A Newton-like learning algorithm, similar to the one presented in Lu *et al* [14] is used to solve the iterative optimization problem of equation-8 to update the estimated vector w:

$$w_{k+1} = w_k - \eta L'_{w_k} / \delta(w_k) \tag{9}$$

where η is the learning rate and

$$\begin{aligned} L'_{w_k} &= \overline{\rho} E\{xG'_y(y)\} - 0.5\mu E\{g'_{w_k}(w_k)\}, \\ \delta(w_k) &= \overline{\rho} E\{xG''_{y^2}(y)\} - 0.5\mu E\{g''_{w_k{}^2}(w_k)\} \end{aligned} \tag{10}$$

Where $\overline{\rho} = \pm\rho$, whose sign is determined by the sign of $E\{G(y)\} - E\{G(y_{Gauss})\}$, $G'_y(y)$ and $G''_{y^2}(y)$ are the first and second derivatives of $G(y)$ with respect to y and $g'_{w_k}(w_k)$ and $g''_{w_k{}^2}(w_k)$ are the first and second derivatives of $g(w)$ with respect to w. The updating is followed by normalization of the vector w:

$$w_{k+1} = w_{k+1} / \|w_{k+1}\| \tag{11}$$

The positivity is then applied by mapping the observed data space via the estimated weighting vector w into the source space, truncating the negative elements of the estimated IC and then re-mapping the IC into the observed data space to get the updated weighting vector w. The Lagrange multiplier is learned by the following gradient ascent method [14].

$$\mu_{k+1} = \max\{0, \gamma g(w_k)\} \tag{12}$$

3. DYNAMIC CONTRAST ENHANCED IMAGE DATA SET ACQUISITION

Adult male Sprague-Dawley rats were anesthetized with isoflurane, tracheotomized and mechanically ventilated. To enable 2PLSM imaging of the brain, stereotaxic surgery was done to prepare a small ($\sim 5mm$ diameter), closed (1% agarose) cranial window over the forelimb representation in the primary somatosensory cortex ($\sim 3.5mm$ lateral to bregma). The tail vein was cannulated to allow administration of the bolus of the fluorescent contrast agent (Texas Red dextran, $70kDa$, $0.05ml$, $25mg/kg$). The rats were anaesthetized to minimize residual motion. Rectal temperature, tidal pressure of ventilation, arterial blood pressure, and heart rate were monitored and recorded using a BIOPAC MP system (Biopac Systems, Inc., Goleta, CA) throughout the experiments. Two-photon microscopy was done using a 20x, 0.95 NA, $2.0mm$ working distance objective (Olympus). The bolus tracking experiments employed a 320×320 matrix over $\sim 600\mu m^2$ field of view, with a 4us dwell time, resulting in $0.366s$ per frame. Figure 1 shows a sample frame of a data set where both artery and vein are visible.

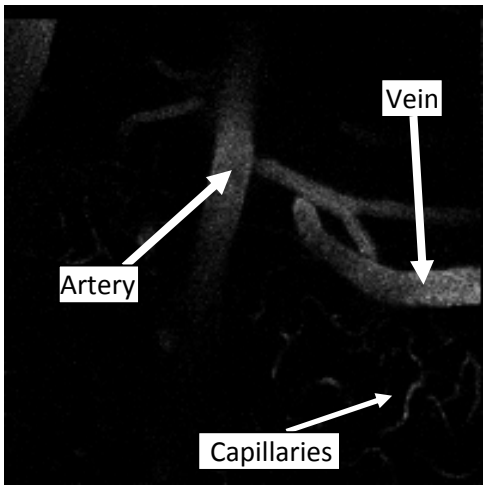

Figure 1. A sample frame of the image data set where artery, vein and small capillaries are visible

4. EXPERIMENT RESULTS

The image sequences are fed to the algorithm and the resulting IC's and component curves are extracted. The results of applying the method to one of data sets is illustrated here. As shown in figure 2 the artery and vein are well separated in temporally constrained ICA (TCICA) method.

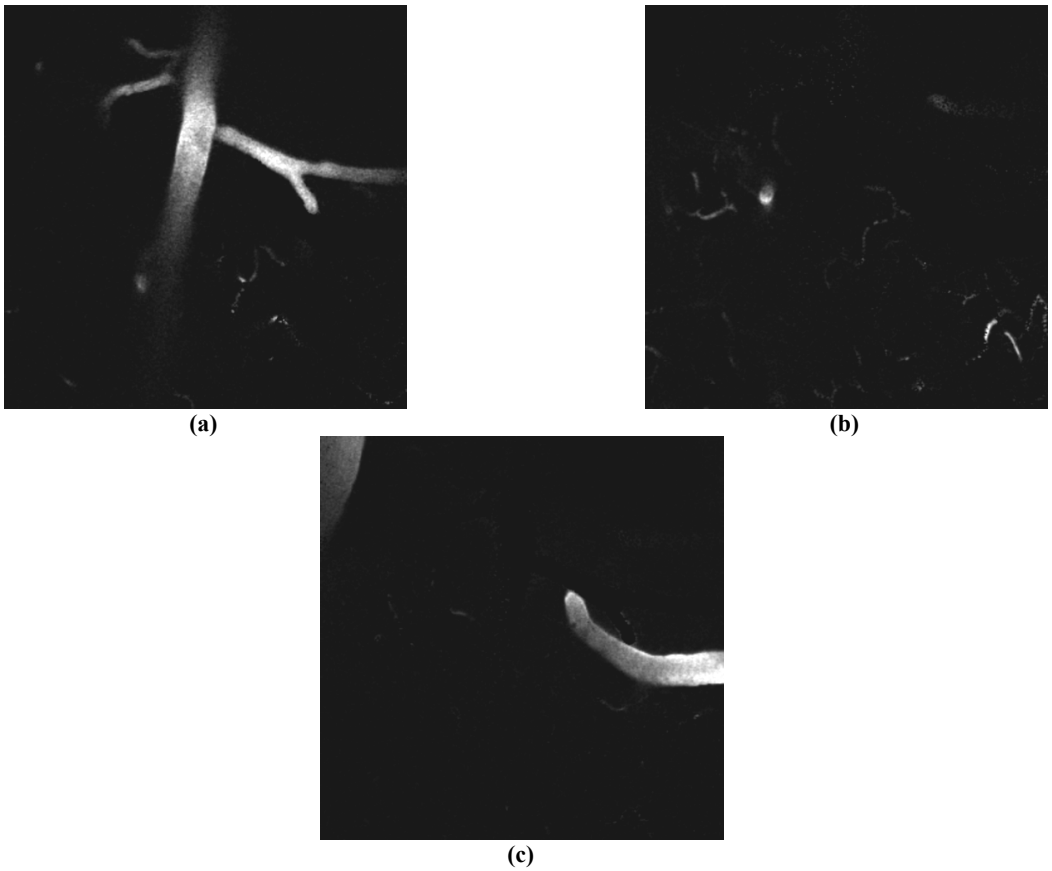

Figure 2. The independent components resulting from applying the TCICA to the rat brain dataset, a) artery, b) capillaries and c) vein

A commonly used classical ICA technique (fast-ICA) as well as pixel by pixel model fitting are also performed to highlight the superior performance of the new algorithm. Figure 3 shows the results of applying fast-ICA to the rat brain data set.

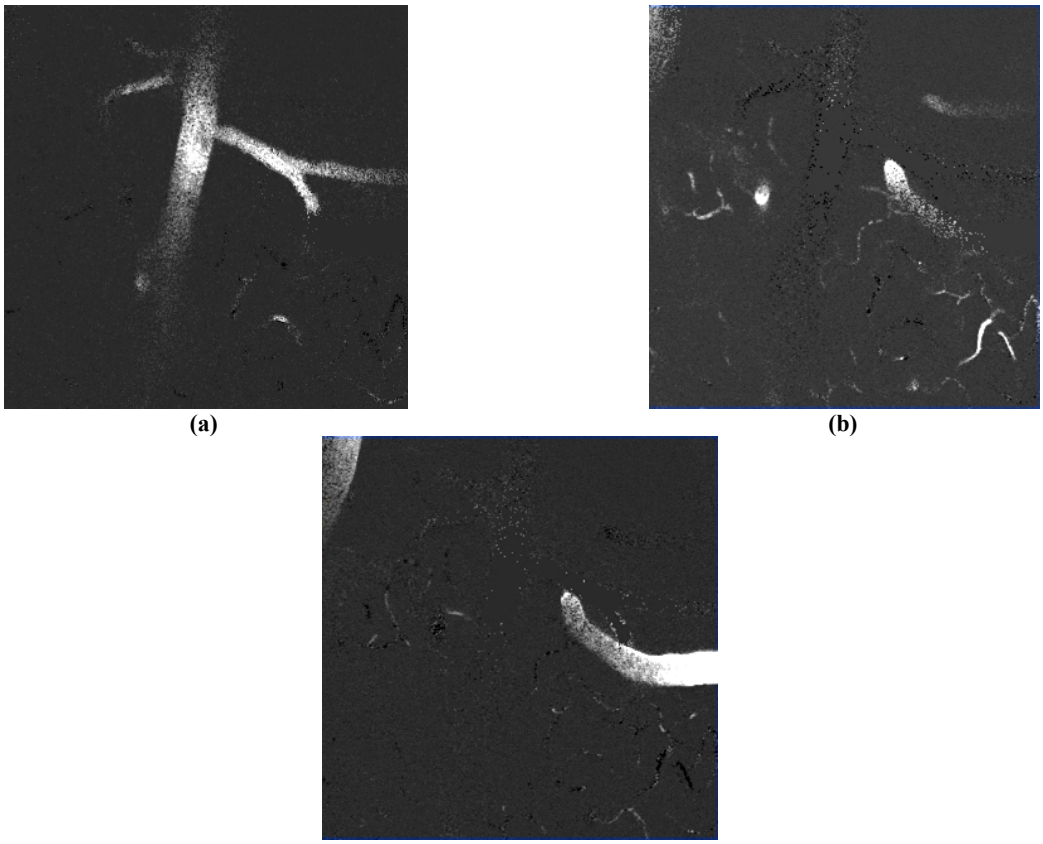

(a) **(b)** **(c)**

Figure 3. The independent components resulting from applying the fast-ICA to the rat brain dataset, a) artery, b)capillaries and c) vein

In figure 4 binary images have been generated from the time to peak map obtained using conventional pixel by pixel model fitting [17]. The histogram of the time to peak map was plotted and 3 peaks were identified; these peaks were used to identify 3 phases and the pixels corresponding to each of the phases are shown in figure 4.

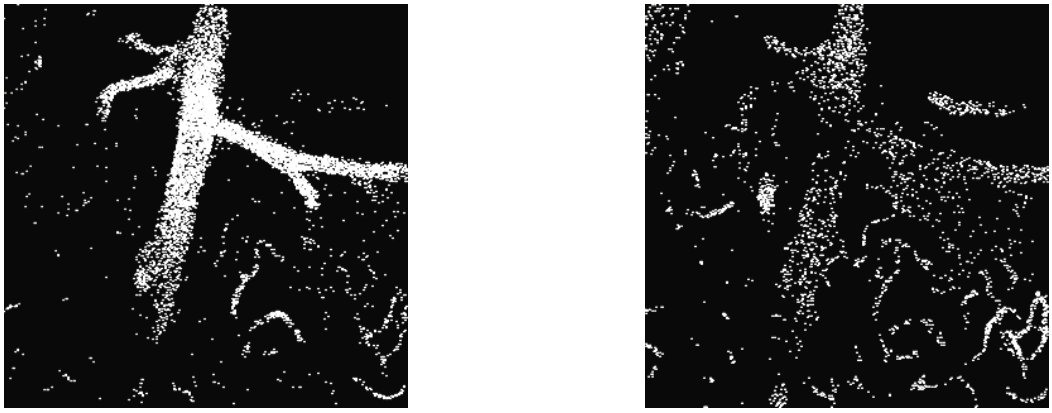

(a) **(b)**

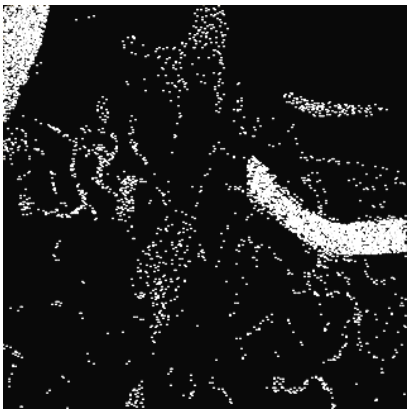

(c)

Figure 4. The binary images generated from the time to peak map obtained using conventional pixel by pixel model fitting of the to the rat brain dataset, a) artery, b) capillaries and c) vein

Figure 5 shows the component curves of the three techniques corresponding to the artery (dashed line), vein (dash-dotted line) and capillaries (solid line).

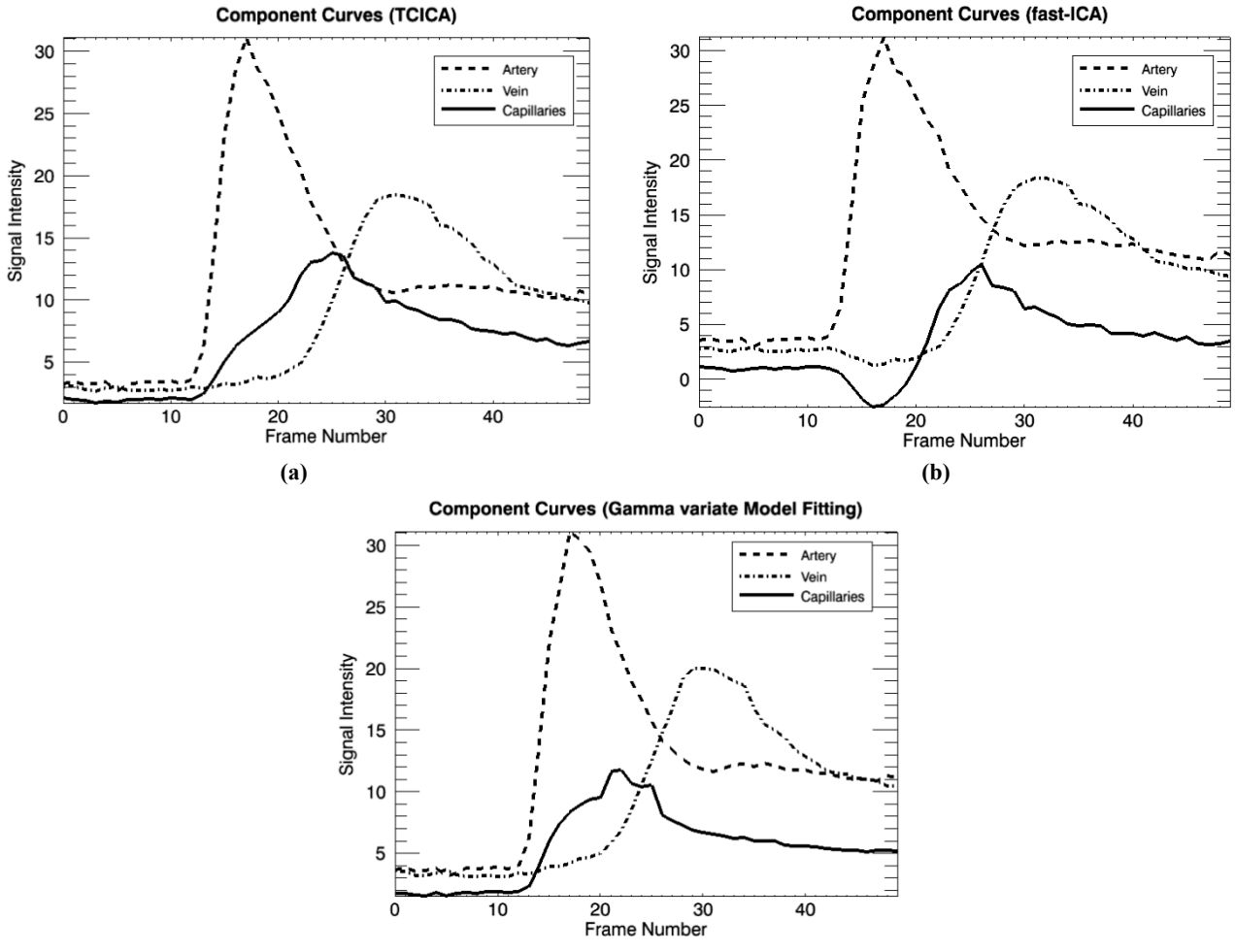

Figure 5. Component curves of a) Constrained ICA b) Classical ICA and c) average fitted gamma variate curve. The dashed line belongs to the artery, the dash-dotted line represents vein and the solid line shows the Capillaries

In table 1 the mean squared error between the normalized component curves and their corresponding gamma variate fits for both TCICA and fast-ICA are given. Table 2 reports the time to peak and table 3 gives the onset time of all three factors of different methods.

Table 1. The mean squared distance of the normalized component curves from their gamma variate fit

	1st Component (Artery)	2nd Component (Capillaries)	3rd Component (Vein)
TCICA	0.0038	0.0077	0.0038
fast-ICA	0.0085	0.0083	0.0048

Table 2. The time to peak extracted from the results of the three methods for each component curve

	1st Component (Artery)	2nd Component (Capillaries)	3rd Component (Vein)
Model Fitting	6.89 (s)	8.42 (s)	11.35 (s)
fact-ICA	6.22 (s)	9.52 (s)	11.71 (s)
TCICA	6.22 (s)	8.42 (s)	11.35 (s)

Table 3. The onset time extracted from the results of the three methods for each component curve

	1st Component (Artery)	2nd Component (Capillaries)	3rd Component (Vein)
Model Fitting	4.76 (s)	4.03 (s)	6.22 (s)
fast-ICA	4.39 (s)	7.32 (s)	8.42 (s)
TCICA	4.39 (s)	6.22 (s)	7.32 (s)

5. DISCUSSIONS

Three different methods, temporally constrained ICA (TCICA), fast-ICA and pixel by pixel gamma variate fitting, are applied to the experimental rat brain microcirculation dataset and the performance of these methods is compared. The proposed TCICA method performed well compared to both the fast-ICA and model based technique. As shown in figure 2 the artery, vein and capillaries are well separated in temporally constrained ICA (TCICA) method as it resulted in less noisy IC's and only small interference from other IC's are present in the extracted component images. Whereas; the results of fast-ICA (figure 3) show that without any regularization, the component images are very noisy and the artery and vein are not separated perfectly, also interference from other IC's are present in the component images. Also, the binary images generated from parametric maps of the pixel by pixel gamma variate curve (figure 4) are very noisy and the artery or vein regions show a lot of interference from other components compared to those obtained using the proposed method (figure 2).

Moreover, the component curves of the fast-ICA technique do not fit well into the gamma variate function while the temporally constrained ICA (TCICA) technique resulted in curves that are closer to gamma variate function as reported in table 1. In addition, as reported in table 2 and table 3, the onset time and time to peak for TCICA compared to fast-

ICA were closer to those of the gamma variate model fitting technique. These tables show the results of temporally constrained ICA match with the model fitting data better than fast-ICA.

The component curves given in figure 5 as well as the component images in figures 2, 3 and 4 show that the data driven techniques perform better in separating the capillaries from artery and vein. This can be seen in the intermediate component (capillaries) curves and also their corresponding component images in each method. These results show the capillaries in the field of view that must also follow a gamma variate function are combined with noise in the model fitting data but they are separated from the background in the data driven techniques. Furthermore, this curve follows a gamma variate function in constrained ICA whereas is has an arbitrary shape in fast-ICA.

6. CONCLUSIONS

Vessel-specific dynamics of cerebral blood flow can be extracted by injecting a bolus of dye into the microvasculature circulatory system and then monitoring its passage through the cerebral microcirculation. The dynamics of the passage of a bolus of dye through artery and vein show clear distinction in onset time, time to peak and dispersion (full-width at half maximum) and therefore artery-vein separation is possible using their dynamic specifications. The conventional way of separation is pixel by pixel model fitting (gamma variate fitting) of the data which is based on *a priori* information about the response of the vasculature (contrast agent concentration in vessels follow a gamma variate function). Model based techniques are very time consuming, sensitive to noise and require specifying region of interest (not automatic).

The goal of this study was to develop a fully automatic data driven technique which incorporates the *a priori* information about the data set as constraints. The first constraint used here is the fact that behavior of the vascular system follows a gamma variate function and the second one is that no negative contribution from arteries and veins are acceptable in constructing the acquired image (positivity constraint). Applying these two constraints to classical ICA technique resulted in a more stable separation algorithm (TCICA).

Experimental study was performed to assess the performance of the temporally constraint ICA (TCICA) technique with the two available analysis techniques for artery-vein separation. TCICA provided better separation of artery, vein and capillaries compared to both methods. Compared to fast-ICA algorithm, TCICA provided physiologically meaningful component curves as its curves better follow gamma variate model and its onset time and time to peak are closer to those of the pixel by pixel model fitting. TCICA also handled noise better than gamma variate model fitting technique as its segmented images were less noisy and better showed the artery, vein and capillaries in the image dataset.

7. ACKNOWLEDGMENTS

The authors would like to thank the Natural Sciences and Engineering Research Council of Canada (NSERC) for supporting this work.

REFERENCES

[1] Wu, X. Y., Liu, G. R., “Independent component analysis of dynamic contrast-enhanced images: The number of components”, Computational Methods, 1111-1116 (2006).
[2] Hutchinson, E. B., Stefanovic, B., Koretsky, A. P., Silva, A. C., “Spatial flow-volume dissociation of the cerebral microcirculatory response to mild hypercapnia”, NeuroImage, **32**, 520-530 (2006).
[3] Tompson, H. K., Starmer, F. C., Whalen, R. E., McIntosh, D., “Indicatior transit time considered as a gamma variate”, Circulation Research, **14**, (June 1964).
[4] Martel, A. L., “A fast method of generating pharmacokinetic maps from dynamic contrast-enhanced images of the breast”, MICCAI, **LNCS 4191**, 101-108 (2006).
[5] Benali, H., Buvat, I., Frouin, F., Bazin, J. P. Di Paola, R., “A statistical model for the determination of the optimal metric in factor analysis of medical image sequences (FAMIS)”, Phys. Med. Biol., **38**, 1065-1080 (1993).
[6] Nijran, K. S., Barber, D. C., “A completely automatic method of processing I-labelled Rose Bengal dynamic liver studies”, Phys. Med. Biol., **31**(5), 563-570 (1986).

[7] Kim, J., Mueller, C. W., [Factor analysis: statistical methods and practical issues], SAGE Publications, chapter II, (1978).
[8] Comon, P., "Independent component Analysis, A new concept?", Signal Processing, 36, 287-314 (1994).
[9] Buvat, I., Benali, H., Frouin, F., Bazin, J. P., Di Paola, R., "Target apex-seeking in factor analysis of medical image sequences", Phys. Med. Biol., **38**(1), 123-38 (Jan 1993).
[10] Barber, D. C., "The use of principal components in a quantitative analysis of gamma camera dynamic studies", Phys. Med. Biol., **25**, 283-292 (1980).
[11] Novey, M., Adali, T., "ICA by Maximization of Nongaussianity using Complex Functions," 2005 IEEE Workshop on Machine Learning for Signal Processing, Art. No. 1532868, 21-26, (2005).
[12] Araujo, A., Giné, E., [The Central Limit Theorem for Real and Banach Valued Random Variables], New York-Chichester-Brisbane-Toronto: Wiley, (1980)
[13] Hyvarinen, A., Oja, E., "Independent Component Analysis: Algorithms and Applications," Neural Networks, **13** (4-5), 411-430,(1999).
[14] Lu, W., Rajapakse, J. C., "Approach and application of constrained ICA", IEEE transaction of Neural Networks, **16** (1), 203-212 (2005).
[15] Shi, Z., Tsng, H., Tang, Y., "A new fixed-point algorithm for independent component analysis" Neurocomputing, **56**, 467-473 (2004).
[16] Lin, Q., Zheng, Y., Yin, F., Liang, H., Calhoun, V. D., "A fast algorithm for one-unit ICA-R", Information Sciences, **177**, 1265-1275 (2007).
[17] Ahearn, T. S., Staff, R. T., Redpath, T. W., and Semple, S. I. K., "The use of the Levenberg–Marquardt curve-fitting algorithm in pharmacokinetic modeling of DCE-MRI data", Phys. Med. Biol., **50**, N85-N95, (2005).